Author(s): Huang, Yun-Hui & Karppinen, Maarit & Imamura, Naoki & Yamauchi, Hisao & Goodenough, John B.

Title: Structural transformation and magnetic competition in Yb(Mn1-xFex)O3

Year: 2007

Version: Final published version

Structural transformation and magnetic competition in Yb(Mn$_{1-x}$Fe$_x$)O$_3$

Yun-Hui Huang,[1,2,*] Maarit Karppinen,[1,3] Naoki Imamura,[1] Hisao Yamauchi,[1] and John B. Goodenough[2]

[1]*Materials and Structures Laboratory, Tokyo Institute of Technology, Yokohama 226-8503, Japan*
[2]*Texas Materials Institute, ETC 9.102, The University of Texas at Austin, Austin, Texas 78712, USA*
[3]*Laboratory of Inorganic and Analytical Chemistry, Helsinki University of Technology, FI-02015 TKK, Finland*

Structural and magnetic properties of the Yb(Mn$_{1-x}$Fe$_x$)O$_3$ ($0 \leq x \leq 1$) system have been systematically investigated. Initial samples were prepared via a sol-gel method. A pure hexagonal phase was only obtained for samples with $x \leq 0.5$. With high-pressure annealing, a pure orthorhombic perovskite phase was achieved for all the compositions. The ^{57}Fe Mössbauer spectrum for $x=0.5$ shows that only Fe^{3+} ions exist in the system; there was no evidence of chemical inhomogeneities. With increasing x, the Néel temperature T_N increases for both hexagonal and orthorhombic phases. The orthorhombic Yb(Mn$_{0.5}$Fe$_{0.5}$)O$_3$ shows an interesting weak ferromagnetic state in the temperature range of 239–298 K, the ferromagnetism disappearing abruptly on cooling below $T_t=239$ K. The transition at T_t appears to be a reorientation of the spin axis of a type-G antiferromagnetic order from the orthorhombic a axis to the b axis in the (010) plane.

I. INTRODUCTION

The RMnO$_3$ oxides of the light rare earths R=La to Dy are orthorhombic perovskites, space group $Pbnm$; for R =Ho to Lu, they are hexagonal, space group $P6_3cm$.[1,2] A high-pressure anneal can transform the hexagonal structure to a metastable orthorhombic perovskite.[3,4] In the orthorhombic structure, a cooperative rotation of the corner-shared MnO$_{6/2}$ octahedra bends the Mn-O-Mn bond angles from 180°, the angle $(180°-\phi)$ decreasing with decreasing radius of the R^{3+} ion. This rotation is accompanied by an intrinsic distortion of the octahedral sites into long O-Mn-O bonds alternating with shorter O-Mn-O bonds in the (001) planes. This distortion biases the cooperative orbital ordering at the high-spin Mn^{3+}: t^3e^1 to give ferromagnetic σ-bond e^1-O-e^0 competing with antiferromagnetic π-bond t^3-O-t^3 spin-spin interactions in the (001) planes.[5] In LaMnO$_3$, the σ-bond component of the spin-spin interactions dominates in the (001) planes; between planes the antiferromagnetic t^3-O-t^3 interactions dominate the spin-spin interactions. Therefore LaMnO$_3$ has type-A antiferromagnetic order with ferromagnetic (001) planes coupled antiparallel to one another.[6] Zhou and Goodenough[7] have shown that as the bias of the cooperative Jahn-Teller orbital ordering from the intrinsic site distortion increases with decreasing R^{3+}-ion radius, the ferromagnetic σ-bond component decreases relative to the antiferromagnetic π-bond component in the (001) planes until, for the heavier rare-earth perovskites stabilized by high-pressure annealing, the two components become comparable in energy. In these perovskites, the competition between the σ-bond and π-bond components is resolved by the stabilization of an exchange-density wave propagating in the [110] direction, ferromagnetic and antiferromagnetic Mn-O-Mn interactions alternating with one another in the (001) planes. This peculiar antiferromagnetic order is labeled type-E. Orthorhombic YbMnO$_3$ has the type-E antiferromagnetic order.

In this paper, we explore the evolution with x of the magnetic transition temperature in the hexagonal and perovskite phases of Yb(Mn$_{1-x}$Fe$_x$)O$_3$. The YbFeO$_3$ perovskite has only antiferromagnetic t^3-O-t^3 and e^2-O-e^2 spin interactions, which gives type-G antiferromagnetic order with a high Néel temperature T_N.[8]

II. EXPERIMENT

Hexagonal Yb(Mn$_{1-x}$Fe$_x$)O$_3$ samples were prepared by a wet-chemical route with stoichiometric amounts of Yb$_2$O$_3$, Fe$_2$O$_3$, and MnCO$_3$ as starting materials and ethylenediaminetetraacetic acid (EDTA) as a complexant, as described elsewhere in detail.[9] The samples were sintered in air at 1200 °C for 20 h. Orthorhombic perovskites were obtained with a high-pressure (HP) technique. The as-prepared samples were each packed in a gold capsule and heated at 1100 °C for 30 min under a pressure of 5 GPa in a cubic-anvil HP apparatus. Our experiments showed that the HP treatment alone without any heating does not give the orthorhombic phase, and a complete transition from the hexagonal to the orthorhombic phase requires an applied pressure of higher than 2 GPa under heating.

The phase purity was checked by x-ray powder diffraction (XRD; Rigaku: RINT-2000 equipped with a rotating copper anode; Cu $K\alpha$ radiation). Lattice parameters were obtained with a Rietveld refinement program, RIETAN 2000. The pattern R factors (R_P) for all the refinements were less than 12%. The XRD data for the refinements were collected at room temperature from 10° to 100° with a 2θ step of 0.02°. Magnetization measurements were made with a superconducting quantum interference device (SQUID; Quantum Design: MPMS-XL5).

For one of the HP-annealed samples, i.e., Yb(Mn$_{0.5}$Fe$_{0.5}$)O$_3$, a ^{57}Fe Mössbauer spectrum was measured to confirm the valence state of iron. The measurement was performed at 350 K in transmission geometry with a Cyclotron Company ^{57}Co:Rh (25 mCi) source. The absorber was prepared by spreading the mixture of the sample with epoxy resin on an Al foil. The spectrum consisting of one broadened doublet peak was fitted with two components of similar
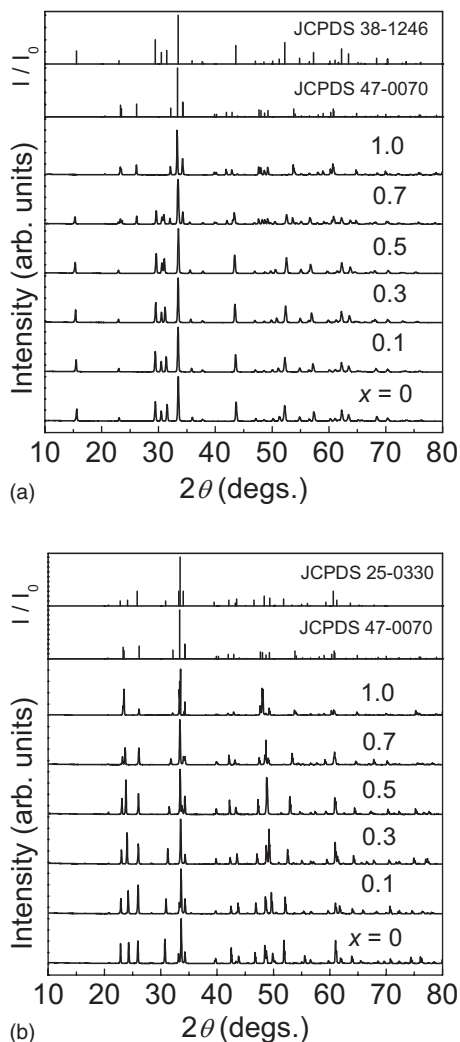
174405-1

FIG. 1. XRD patterns for $Yb(Mn_{1-x}Fe_x)O_3$ with $x=0$, 0.1, 0.3, 0.5, 0.7, and 1.0: (a) sintered at 1200 °C for 20 h in air, and (b) further annealed at 1100 °C for 30 min under a pressure of 5 GPa.

FIG. 2. Lattice parameters for (a) hexagonal and (b) orthorhombic $Yb(Mn_{1-x}Fe_x)O_3$ samples.

isomer shift (IS) values to account for the broadening. The broadening is due to random distribution of Fe and Mn atoms, which causes the local quadrupole coupling constant to vary.[10]

III. RESULTS AND DISCUSSION

Room-temperature XRD patterns in Fig. 1 showed that the initial samples exhibited a pure hexagonal $P6_3cm$ phase for $x \leq 0.5$ (JCPDS No. 38-1246), mixed hexagonal and orthorhombic *Pbnm* perovskite phases for $0.6 \leq x \leq 0.8$, and a pure orthorhombic perovskite for $x=1.0$ (JCPDS No. 47-0070). Due to the Jahn-Teller effect of Mn^{3+} and the small ionic radius of Yb^{3+}, the noncentrosymmetric hexagonal structure is preferred for $YbMnO_3$ under ambient pressure. Yb^{3+} ions are situated at two different sites $2a$ and $4b$. Fivefold-coordinated Mn^{3+} ions are located at the $6c$ site surrounded by a trigonal bipyramid of O^{2-} ions; they form a triangular network within a hexagonal c plane. With substitution of Fe^{3+} for Mn^{3+}, the structure strongly depends on the
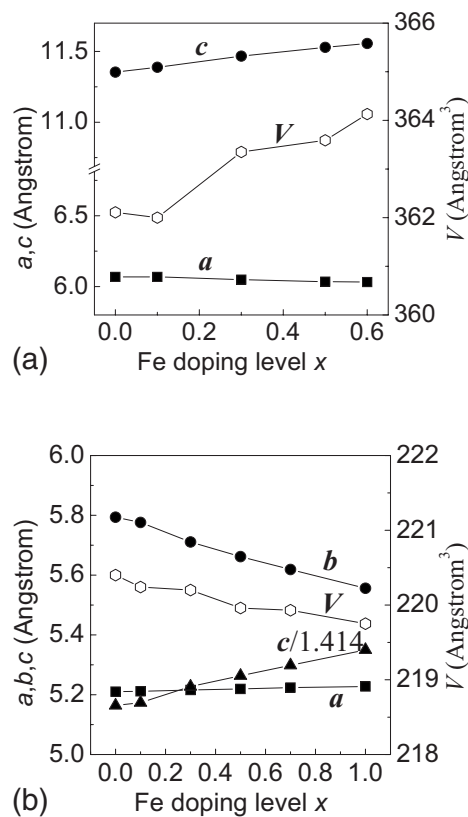
Fe^{3+} doping level x. However, after HP annealing, a pure orthorhombic perovskite phase (JCPDS No. 25-0330 for smaller x and 47-0070 for larger x) was obtained for all values of x, see Fig. 1. The structural transformation from hexagonal to orthorhombic phase by high-pressure treatment is because of the pressure-induced change in density and hence reconstruction of the lattice.[11] High pressure prefers the structure with a high symmetry and a high density, which causes the coordination of Mn^{3+} ions to change from fivefold to sixfold. The lattice parameters obtained by Rietveld refinement are displayed in Fig. 2. An obvious change in the lattice parameters with Fe doping level x occurs in both hexagonal and orthorhombic series. The ^{57}Fe Mössbauer spectrum in Fig. 3 of the orthorhombic $Yb(Mn_{0.5}Fe_{0.5})O_3$ perovskite phase (with a line broadening associated with different numbers of Mn^{3+}-ion near neighbors) shows that the isomer shift value ($\sim$0.32 mm/s) is close to that typical of Fe^{3+} ions.

Figure 4 displays the temperature dependence of the zero-field-cooled (ZFC) and field-cooled (FC) magnetic susceptibility $\chi(T)$ measured on heating in 100 Oe for both as-prepared $Yb(Mn_{1-x}Fe_x)O_3$ samples and those obtained by the HP anneal. The rapid increase in $\chi(T)$ at low temperatures reflects the paramagnetic contribution to $\chi(T)$ from the Yb^{3+} ions. The long-range magnetic-ordering temperatures are difficult to be defined clearly from the $\chi(T)$ curves for some samples, so we show in Fig. 5 the curves $d\chi/dT$. As shown previously,[9] the anomaly at 88 K in hexagonal $YbMnO_3$ is
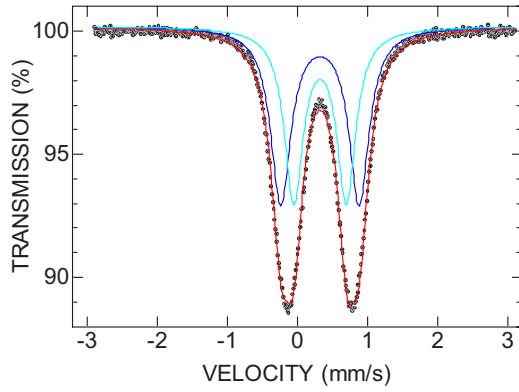
FIG. 3. (Color online)[57]Fe Mössbauer spectrum at 350 K for the orthorhombic $Yb(Mn_{1-x}Fe_x)O_3$, fitted with two components with essentially identical isomer-shift values of 0.32 and 0.33 mm/s.

due to a canted spin ordering of the Mn^{3+} ions. This T_N increases progressively to 112 K with increasing x in hexagonal $Yb(Mn_{1-x}Fe_x)O_3$ $(0 \leq x \leq 0.5)$. In the as-prepared x =0.6 and 0.7 samples, the T_N of the hexagonal phase remains fixed at the value for $x=0.5$, which signals that the composition limit of the hexagonal phase is about $x=0.5$. For the orthorhombic HP samples, the type-E antiferromagnetic T_N =43 K for $x=0$ increases to $T_N=62$ K for $x=0.4$. The orthorhombic $x=0.5$ sample exhibits a completely different magnetic behavior; it shows a weak ferromagnetic state in the temperature range of 239–298 K below an apparent Néel temperature at $T_N=298$ K; the weak ferromagnetic state is followed by an abrupt transition to an antiferromagnetic phase below $T_t=239$ K. An anomaly at 8 K is ascribed to an ordering of Yb^{3+} spins as confirmed in our previous work;[9] it can also be observed in the other $Yb(Mn_{1-x}Fe_x)O_3$ samples. As x increases further, the onset of long-range magnetic order increases to above 350 K and the transition at T_t gets weaker, disappearing in the $x=0.8$ and 1.0 samples.

To determine further the magnetic state of the orthorhombic $x=0.5$ sample, we measured magnetization (M) as a function of magnetic field (H) at various temperatures. As shown in Fig. 6, the M-H curves from 230 to 300 K exhibit an almost linear relationship, being dominated by the paramagnetic susceptibility of the Yb^{3+} ions. However, an M-H hysteresis loop can be observed at a temperature 250 K
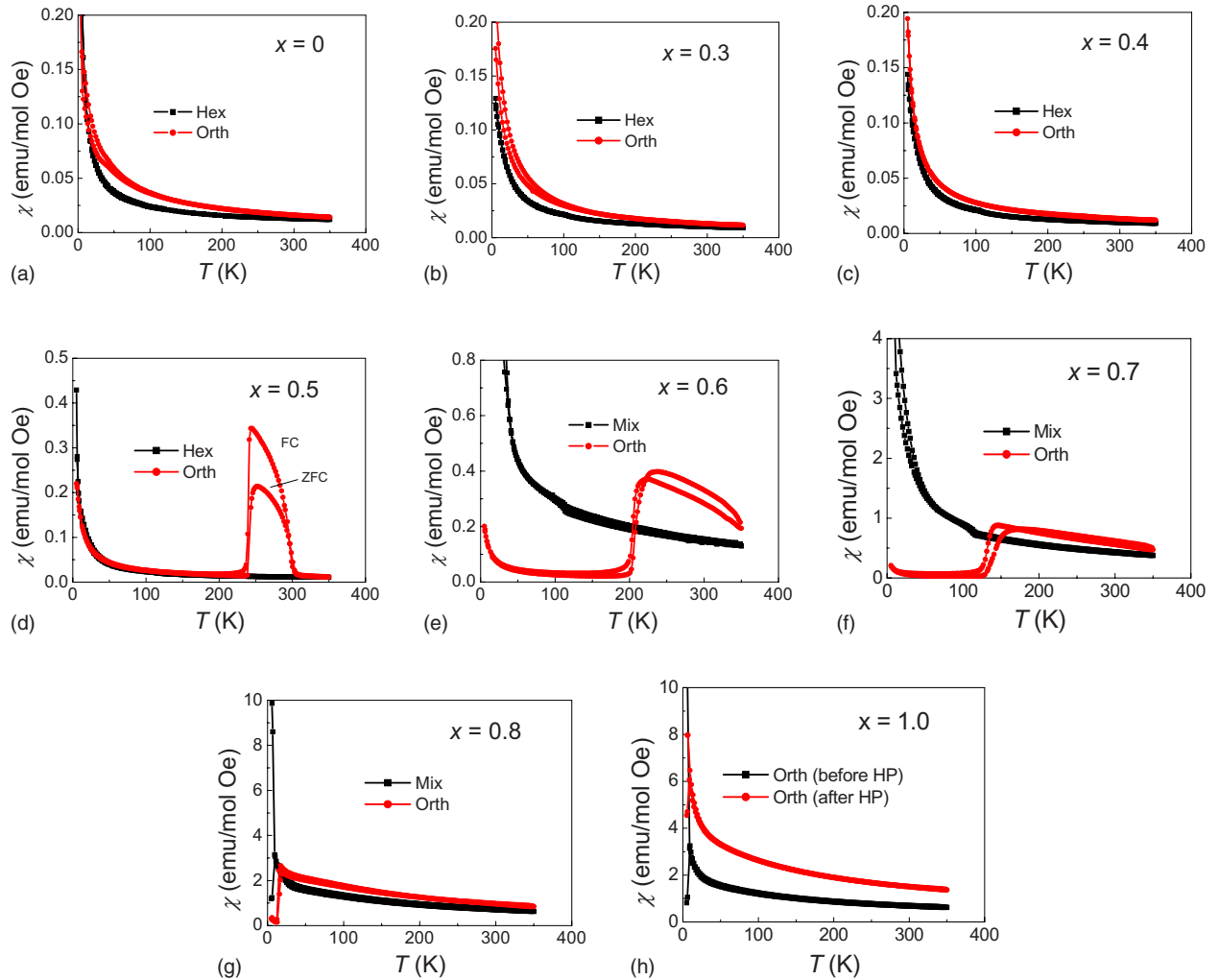

FIG. 4. (Color online) Temperature dependence of zero-field-cooled (ZFC) and field-cooled (FC) susceptibility (χ) measured under a field of 100 Oe for $Yb(Mn_{1-x}Fe_x)O_3$ with $x=0-1.0$ (Hex: hexagonal phase without HP annealing; Mix: mixed hexagonal and orthorhombic phases without HP annealing; and Orth: orthorhombic phase obtained via HP annealing).
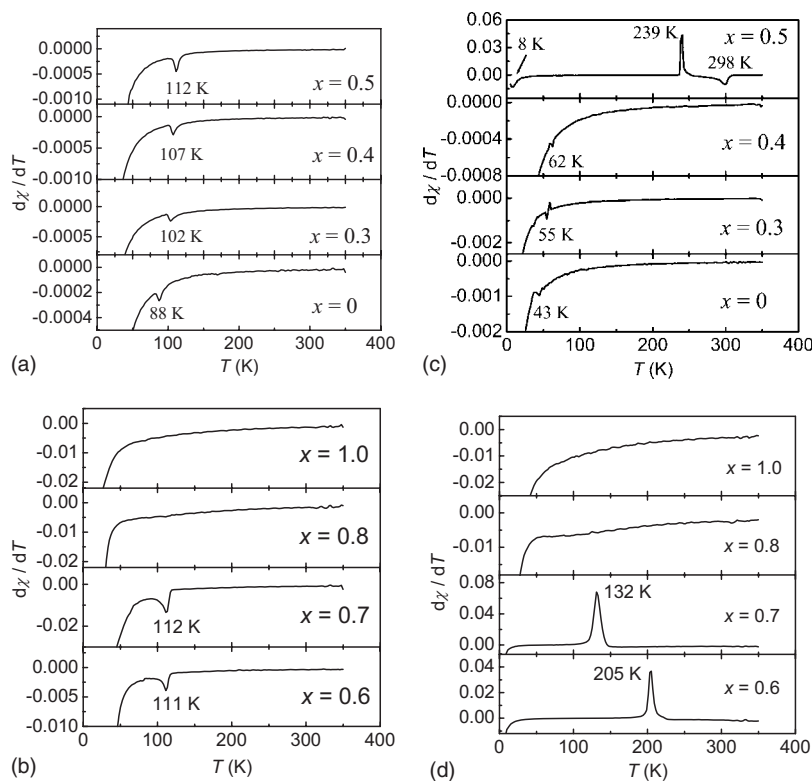
FIG. 5. $d\chi/dT$ as a function of temperature for (a) and (b) hexagonal and (c) and (d) orthorhombic Yb(Mn$_{1-x}$Fe$_x$)O$_3$ with $x=0-1.0$.

where the weak ferromagnetism is large (see the inset A of Fig. 6). The weak ferromagnetic component causes only a small shift in the Weiss constant. After subtraction from the measured magnetization of the paramagnetic component caused by the Yb^{3+} ions, we obtained the contribution from the transition-metal ions. The as-obtained result is shown in the inset B. The *M-H* hysteresis loop becomes more obvious in inset B; it has a small saturation magnetization in a field of

FIG. 6. (Color online) Field-dependent magnetization for the orthorhombic Yb(Mn$_{0.5}$Fe$_{0.5}$)O$_3$ at different temperatures; the inset A shows the magnetic hysteresis loop at 250 K, and the inset B shows the hysteresis loop obtained by subtraction of the paramagnetic component of Yb^{3+} ions.

5 T and a large coercivity $H_c \approx 1.8$ kOe. This result clearly indicates that the orthorhombic $x=0.5$ sample exhibits a weak ferromagnetism.

The hexagonal structure of YbMnO$_3$ contains Mn^{3+} ions at trigonal-bipyramidal $6c$ sites and Yb^{3+} ions at $2a$ and $4b$ sites. The Mn^{3+} ions form a triangular network in the (001) planes, and the axes of the trigonal-bipyramidal sites are canted with respect to the c axis. For a given triangle of Mn^{3+} ions, the projections of the canting are at 120° with respect to one another. These cantings displace the Yb^{3+} ions along the c axis from the centers of their interstices, the Yb^{3+} ions at $4b$ sites moving opposite to those at the $2a$ sites to give a ferrielectric transition below a $T_c \approx 1000$ K.[12] The antiferromagnetic spin-spin interactions in the Mn planes are frustrated, which makes the antiferromagnetic order below $T_N=88$ K noncollinear. The canting of the Mn^{3+}-ion spins is enhanced by exchange striction below T_N to give a coupling of the magnetic order to the ferrielectric polarization, which makes the hexagonal phase multiferroic.[13]

The tabulated ionic radii for the Fe^{3+} and Mn^{3+} ions are essentially the same, but the Mn^{3+} ions, with a $3d^4$ half-shell, are more stable than the Fe^{3+} ions at the trigonal-prismatic sites of the hexagonal structure. Therefore the hexagonal RFeO$_3$ phase is not found in the bulk state; it has only been obtained as nanoparticles for Eu and Yb and as epitaxial films for Eu-Lu.[14,15] The increase with x in the c lattice parameter of the hexagonal phase in Fig. 2, but not the a parameter, shows that the hole in the $3d^4$ half-shell of the Mn^{3+} ion occupies the $3z^2-r^2$ orbital. In contrast to the hexagonal phase, the volume of the orthorhombic phase decreases with increasing x. In orthorhombic YbMnO$_3$, a $c/\sqrt{2}<a$ signals a cooperative antiferroic Jahn-Teller orbital ordering, but the
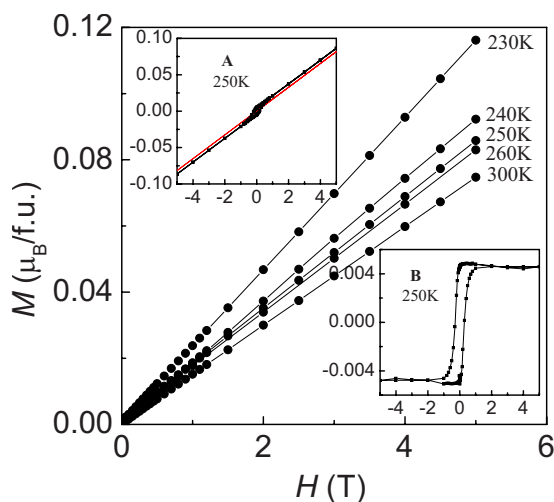
type-E antiferromagnetic order below $T_N=43$ K shows a competition between ferromagnetic σ-bond and antiferromagnetic π-bond spin-spin interactions. In YbFeO$_3$, there is no orbital ordering, so $c/\sqrt{2}>a$ is found and strong antiferromagnetic e^2-O-e^2 (Fe-O-Fe) interactions between nearest neighbors order the Fe^{3+}-ion spins at room temperature. As Fe^{3+} is substituted for Mn^{3+} with increasing x, the cooperative orbital ordering is progressively made less stable, so $c/\sqrt{2}$ increases relative to the a axis.

The iron spins couple much more strongly to neighboring spins than do the Mn^{3+} ions, so T_N increases progressively with x in the hexagonal phase for $x\leq0.5$. A similar increase in T_N with $x\leq0.4$ is found for the orthorhombic phase; but an abrupt change in the internal $0.4<x<0.5$ shows that the long-range cooperative orbital ordering at the Mn^{3+} ions disappears by $x=0.5$. With the disappearance of long-range, static orbital order, a dynamic Jahn-Teller site deformation can be expected to remain. There is, therefore, no reason to assume anything other than antiferromagnetic nearest-neighbor interactions and a type-G magnetic order for $0.5\leq x\leq1.0$ in the orthorhombic phase. A type-G magnetic order has a Dzialoshinskii vector D_{ij} along the axis of the cooperative octahedral-site rotations, i.e., the b axis in *Pbnm*. In this case, the antisymmetric exchange term $D_i \cdot S_i \times S_j$ gives a weak ferromagnetic component due to spin canting if the spins are in the (001) plane perpendicular to b, but no ferromagnetic component if the spins are parallel to the b axis.[16] Since the ferromagnetic component remains weak and Mössbauer data show no evidence of chemical inhomogeneity, we conclude that the peculiar magnetization curves in the interval $0.5\leq x\leq0.7$ of Fig. 4 reflect a canted-spin weak ferromagnetism in the interval $T_t\leq T\leq T_N$ with a reorientation of the spin axes to the b axis below T_t.

IV. CONCLUSIONS

With substitution of Fe^{3+} for Mn^{3+}, stable hexagonal Yb(Mn$_{1-x}$Fe$_x$)O$_3$ samples can be obtained for $x\leq0.5$. High-pressure annealing can completely transform the hexagonal phase to the orthorhombic perovskite for all the compositions with $0\leq x<1$. For the compounds with the same composition, the hexagonal phase and the orthorhombic perovskite show totally different magnetic behaviors. The hexagonal Yb(Mn$_{1-x}$Fe$_x$)O$_3$ samples are antiferromagnetic at low temperatures with a canted-spin ordering of the frustrated Mn^{3+} spins. Their T_N values increase with x in the range $0\leq x\leq0.5$. The perovskite series shows an interesting magnetic phase diagram. Type-E antiferromagnetic $T_N=43$ K for $x=0$ increases to $T_N=62$ K for $x=0.4$, but the $x=0.5$ sample exhibits a weak ferromagnetism below a Néel temperature $T_N=298$ K followed by an abrupt loss of the weak ferromagnetism below $T_t=239$ K. The magnetic behavior for $x\geq0.5$ is characteristic of type-G antiferromagnetic order. Further increases in x give rise to an increase of T_N and a decrease of T_t, which disappears at $x=0.8$ and 1.0.

*yunhuihuang@yahoo.com

[1] H. L. Yakel, Acta Crystallogr. **8**, 394 (1955).

[2] H. L. Yakel, W. C. Koehler, E. F. Bertaut, and E. F. Forrat, Acta Crystallogr. **16**, 957 (1963).

[3] A. Waintal, J. J. Capponi, E. F. Bertaut, M. Contré, and D. Francois, Solid State Commun. **4**, 125 (1966).

[4] A. Waintal and J. Chevanas, Mater. Res. Bull. **2**, 819 (1967).

[5] J. B. Goodenough, Phys. Rev. **100**, 564 (1955).

[6] E. O. Wollan and W. C. Koehlor, Phys. Rev. **100**, 545 (1955).

[7] J. S. Zhou and J. B. Goodenough, Phys. Rev. Lett. **96**, 247202 (2006).

[8] A. Bombik, B. Leśniewska, J. Mayer, and A. W. Pacyna, J. Magn. Magn. Mater. **257**, 206 (2003).

[9] Y. H. Huang, H. Fjellvåg, M. Karppinen, B. C. Hauback, H. Yamauchi, and J. B. Goodenough, Chem. Mater. **18**, 2130 (2006).

[10] E.-L. Rautama, J. Lindén, H. Yamauchi, and M. Karppinen, J. Solid State Chem. **180**, 440 (2007).

[11] J.-S. Zhou, J. B. Goodenough, J. M. Gallardo-Amores, E. Morán, M. A. Alario-Franco, and R. Caudillo, Phys. Rev. B **74**, 014422 (2006).

[12] T. Lonkai, D. G. Tomuta, U. Amann, J. Ihringer, R. W. Hendrikx, D. M. Tobbens, and J. A. Mydosh, Phys. Rev. B **69**, 134108 (2004).

[13] H. D. Zhou, J. C. Denyszyn, and J. B. Goodenough, Phys. Rev. B **72**, 224401 (2005).

[14] Y. Mizoguchi, H. Onodera, H. Yamauchi, M. Kagawa, Y. Syono, and T. Hirai, Mater. Sci. Eng., A **217/218**, 164 (1996).

[15] A. A. Bossak, I. E. Graboy, O. Y. Gorbenko, A. R. Kaul, M. S. Kartavtseva, V. L. Svetchnikov, and H. W. Zandbergen, Chem. Mater. **16**, 1751 (2004).

[16] E. E. Bertant, *Magnetism: A Treatise on Modern Theory and Materials*, edited by E. J. Rado and H. Suhl (Academic Press, New York, 1963).